MECHANICAL ENGINEERING AND SOLID MECHANICS SERIES

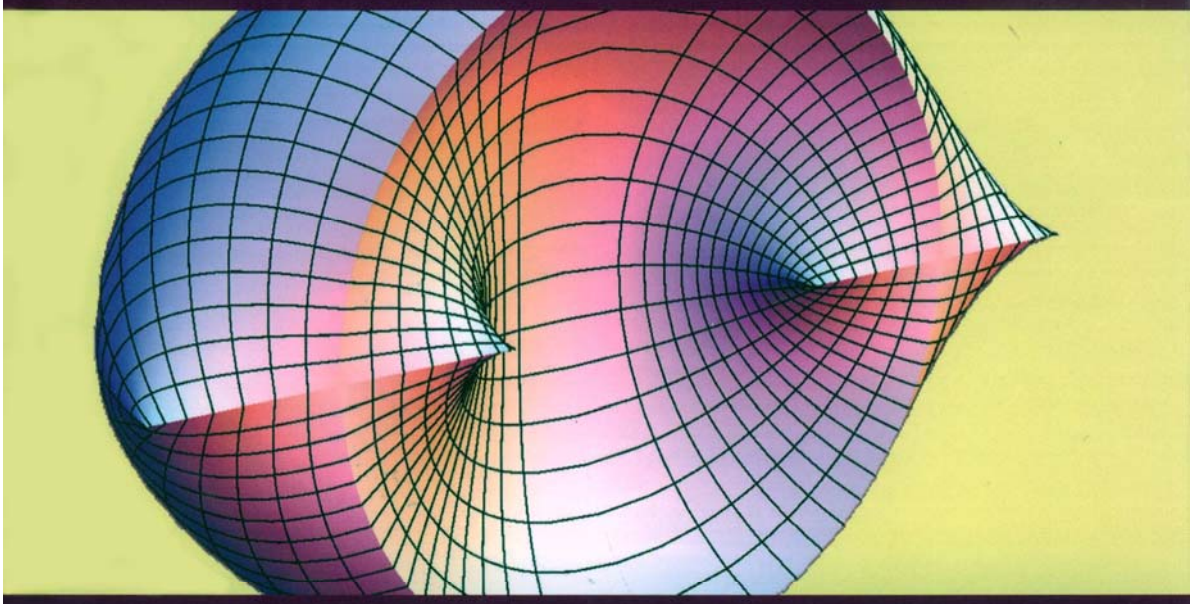

Nonlinear Physical Systems

Spectral Analysis, Stability and Bifurcations

Edited by
Oleg N. Kirillov
Dmitry E. Pelinovsky

iSTE WILEY

Nonlinear Physical Systems

Spectral Analysis, Stability and Bifurcations

Edited by
Oleg N. Kirillov
Dmitry E. Pelinovsky

Series Editor
Noël Challamel

ISTE

WILEY

First published 2014 in Great Britain and the United States by ISTE Ltd and John Wiley & Sons, Inc.

ISTE Ltd
27-37 St George's Road
London SW19 4EU
UK

www.iste.co.uk

John Wiley & Sons, Inc.
111 River Street
Hoboken, NJ 07030
USA

www.wiley.com

Library of Congress Control Number: 2013950133

British Library Cataloguing-in-Publication Data
A CIP record for this book is available from the British Library
ISBN: 978-1-84821-420-0

Printed and bound in Great Britain by CPI Group (UK) Ltd., Croydon, Surrey CR0 4YY

Table of Contents

Preface

The BIRS Workshop on *Spectral Analysis, Stability and Bifurcations in Modern Nonlinear Physical Systems*[1] brought together a unique combination of experts in modern dynamical systems, mathematical physics, partial differential equations (PDEs), numerical analysis, operator theory and applications.

One of the immediate outcomes of the meeting is this post-conference volume of papers from the participants of the workshops making its materials available to a wider audience. This book presents unique viewpoints of the participants on the history, current state of the art and prospects of research in their fields contributing to the progress of stability theory. In this book, we have compiled a collection of essays – mathematical, physical and mechanical. The contributions show connections between different approaches, applications and ideas. We believe that such a book could set the benchmarks and goals for the next generation of researchers and be a true event in modern stability theory. The other outcomes will be seen over a long period of time, when the ideas formulated and discussed during the workshop, as well as new collaborations made, will lead to new scientific publications and new research discoveries.

This book covers the problems of spectral analysis, stability and bifurcations arising from the nonlinear PDEs of modern physics. Bifurcations and stability of solitary waves, stability analysis in hydro- and magnetohydrodynamics and dissipation-induced instabilities will be treated with the use of the theory of Krein and Pontryagin space, index theory, the theory of multiparameter eigenvalue problems and modern asymptotic and perturbative approaches. All chapters contain mechanical and physical examples and combine both tutorial and advanced sections,

1 Took place at the Banff International Research Station for Mathematical Innovation and Discovery, Banff, Canada on 4–9 November 2012. For more information see http://www.birs.ca/events/2012/5-day-workshops/12w5073.

making them attractive both to professionals working in the field and non-specialists interested in knowing more about modern methods and trends in stability theory.

Chapter 1, written by Davide Bigoni and his colleagues, opens the book and presents the reader with sophisticated experiments with simple mechanical structures demonstrating buckling under tensile dead loading (without elements subject to compression at all) and flutter or oscillatory instability of a two-link pendulum that is caused by Coulomb friction. This new look at the classical mechanics is directly motivated by the successes of modern materials science.

The semi-classical n-dimensional quantum tunneling effect, through a hyperbolic fixed point, is treated by Jean-François Bony *et al.* in Chapter 2. The transfer operator which solves this microlocal Cauchy problem appears to be a Fourier integral operator which gives outgoing waves in terms of incoming waves. As an application, the longtime behavior of the Schrödinger group at barrier top is described in term of resonances with explicit generalized spectral projections. Another application is to obtain resonances free regions for homoclinic trapped sets.

A semi-classical limit of a quantum problem on angular momenta interacting in a magnetic field has led Richard Cushman and his colleagues to a curious one-parameter family of Hamiltonian systems in Chapter 3. Their system exhibits an S^1-equivariant sign exchange bifurcation in its linearization about an equilibrium point. The stability of this bifurcation under small S^1-invariant perturbations by linear Hamiltonian vector fields is shown in an instructive manner involving the method of versal deformations.

In Chapter 4, Olivier Doaré discusses the counter-intuitive destabilizing effect of damping in the problems of fluid–structure interaction. A model problem considered is a fluid–conveying pipe where the viscous damping is shown to destabilize the negative energy waves. The fluid-conveying pipe is a model problem for many fluid-elastic systems where a compliant structure interacts with a flow, such as flags, plates, shells, walls or wings. The model is of particular interest in the modern energy-harvesting applications.

Sergey Dobrokhotov and Anatoly Anikin discuss in Chapter 5 the splitting of the lowest eigenvalues of the multidimensional Schrödinger operator with the double-well potential. As a rule, the splitting formula is based on the instanton, which is a singular trajectory of the Newtonian system with inverted potential. However, a physically relevant form of the formula should involve, as the authors demonstrate, not the instanton but an appropriate unstable periodic trajectory (libration).

Periodic potentials and solitons are the subject of Chapter 6, written by Nir Dror and Boris Malomed. To stabilize the solitons in a two-dimensional Bose-Einstein condensate, a linear periodic potential is induced by means of the optical lattices, which are the interference patterns created by laser beams shone through the

condensate. Such periodic potentials give rise to bandgaps in the corresponding linear spectrum, which, in combination with the self-focusing or self-defocusing nonlinearity, support various types of localized mode. The authors demonstrate that bound complexes built of the dipole solitons, in the form of bi-dipoles and four-dipole non-topological states, vortices and quadrupoles, are all stable if the underlying dipole is stable.

A steady Euler flow of an inviscid incompressible fluid is characterized as an extremum of the total kinetic energy with respect to perturbations constrained to an isovortical sheet. Yasuhide Fukumoto *et al.* analyze in Chapter 7 the criticality in the Hamiltonian to calculate the energy of three-dimensional waves on a steady vortical flow and to calculate the mean flow induced by nonlinear interaction of waves with themselves. The energy of waves on a rotating flow is expressible in terms of a derivative of the dispersion relation with respect to the frequency.

Pure imaginary eigenvalues in 1:1 semi-simple resonance (diabolical points in the physics language) typically occur in rotationally symmetrical non-dissipative models of physics and engineering. Its unfolding caused by symmetry-breaking and non-conservative perturbation is a reason for many instabilities such as the rotating polygon instability of swirling free surface flow. In Chapter 8, Igor Hoveijn and Oleg Kirillov map all possible singularities on the boundary of the stability domain of perturbed four-dimensional systems in 1:1 resonance and apply the result to the study of the enhancement of the modulation instability with dissipation.

Since the time of the celebrated Kelvin–Tait–Chetaev theorem, counts of unstable point spectra and other related counts that are referred to as index theorems have appeared across various distinct and unrelated fields due to their simple structure and importance for stability applications. Richard Kollár and Radomír Bosák give in Chapter 9 a unique and comprehensive survey of the index theorems motivated by very different physical, algebraic and control theory applications and also present a graphical Krein signature theory. The latter makes the proofs of index theorems for linearized Hamiltonians extremely elegant in the finite dimensional setting: a general result implying Vakhitov–Kolokolov criterion (or Grillakis–Shatah–Strauss criterion) as a corollary generalized to problems with arbitrary kernels, and a count of real eigenvalues for linearized Hamiltonian systems in canonical form.

Chapter 10 provides an example of counting unstable eigenvalues in the problems of vortex dynamics presented by Paolo Luzzatto-Fegiz and Charles H.K. Williamson. They demonstrate that the turning points in impulse of the vortex array correspond to a change in the number of unstable modes. Furthermore, whether the isovortical rearrangements involve the introduction or removal of an unstable mode can be inferred from the shape of a fold in the phase velocity–impulse plot.

In Chapter 11, the fluid dynamical theme is continued by Sherwin Maslowe who provides a general and comprehensive survey of the finite amplitude theory and discusses in detail the critical layer analyses that indicate, in particular, important resolution requirements for computational schemes.

A main motivation for studying Hamiltonian systems is their universality. In Chapter 12, Philip Morrison and George Hagstrom show how infinite-dimensional noncanonical Hamiltonian systems enlarge this universality class. Any specific system within the classes of systems considered may possess steady-state bifurcations, positive and negative energy modes and Krein's theorem for the Hamiltonian Hopf bifurcations. An analogous situation transpires for the continuous steady-state and Hamiltonian Hopf bifurcations. However, continuous spectra are difficult to deal with mathematically and functional analysis is essential. For example, we can interpret the continuous Hamiltonian Hopf bifurcation as the Hamiltonian Hopf bifurcation with the second mode coming from the continuous spectrum. Chapter 12 sets the stage for the explicit treatment of bifurcations with the continuous spectrum that is considered in Chapter 13.

A hybrid fluid-kinetic model of plasma physics considered by Philip Morrison and his coauthors in Chapter 14 combines a magnetohydrodynamics (MHD) part for a description of bulk fluid components and a Vlasov kinetic theory part that describes an energetic plasma component. In the considered model, a Hamiltonian structure is found that allows the authors to implement the energy-Casimir method for an explicit derivation of sufficient stability conditions.

Semigroups (or dynamical systems) of contractions in Hilbert space with non-self-adjoint generators considered by Francis Nier in Chapter 15 are motivated by the linearization of incompressible 2D-Navier-Stokes equation in the vortex formulation around Oseen vortices and by the Feller semigroup associated with the Langevin dynamics, which solves the Kramers–Fokker–Planck equation. The accurate estimates for the exponential decay of such semigroups with parameter-dependent non-self-adjoint generators obtained by the author substantially involve the theory of pseudo-spectrum.

The theory of pseudo-spectrum reappears in Chapter 16 where Michael Overton gives a broad survey of recent achievements in stability optimization for polynomials and matrices. The optimization problems discussed in this chapter typically lead to optimizers that are polynomials with multiple roots or matrices with non-derogatory multiple eigenvalues. The higher their multiplicity, the more these multiple roots or eigenvalues are sensitive to small perturbations; furthermore, computing these minimizers numerically is difficult. Instead of optimizing eigenvalues it is proposed to consider optimization of the pseudo-spectral radius and pseudo-spectral abscissa, which is computationally less difficult than for the spectral radius and spectral abscissa.

In Chapter 17, Dmitry Pelinovsky returns to the index theory and proves the index theorem in a rather general setting motivated by the problems of stability of nonlinear waves in KdV-type evolution equations. The directions leading to further extensions of this result are pointed out.

In the final Chapter 18, Zensho Yoshida and Philip Morrison describe several facets of noncanonical Hamiltonian systems, namely, the Poisson operator (field tensor) of a noncanonical Hamiltonian system has a non-trivial kernel (and thus, a cokernel) that foliates the phase space (Poisson manifold), imposing topological constraints on the dynamics. When we can "integrate" the kernel of the Poisson operator to construct Casimir elements, the Casimir leafs foliate the Poisson manifold and, then, the effective energy is the energy-Casimir functional. The theory is applied to the tearing-mode instability, where a tearing mode is regarded as an equilibrium point on a helical-flux Casimir leaf. As long as the helical-flux is constrained, the tearing mode cannot grow. However, it is shown that a singular perturbation that allows the system to change the helical flux can cause a tearing mode to grow if it has an excess energy with respect to a fiducial energy of the Beltrami equilibrium at the bifurcation point.

Oleg N. KIRILLOV
Dmitry E. PELINOVSKY
October 2013

Chapter 1

Surprising Instabilities of Simple Elastic Structures

In this chapter, examples of structures buckling in tension are presented, where no compressed elements are present, slightly different from those previously proposed by the authors. These simple structures exhibit interesting postcritical behaviors; for instance, multiple configurations of vanishing external force are evidenced in one case. Flutter instability as induced by dry friction is also considered in the Ziegler pendulum, with the same arrangement presented by Bigoni and Noselli [BIG 11], but now considering the dynamical effects due to the mass of the wheel, which was previously neglected. It is shown that, for the values of rotational inertia pertinent to our experimental setup, this effect does not change the overall behavior, so that previous results remain fully confirmed.

1.1. Introduction

The first example of an elastic structure buckling for a tensile dead load, without elements subject to compression, has been provided by Zaccaria *et al.* [ZAC 11]. This finding opens new possibilities in the design of compliant structures. In this chapter, we present a single-degree-of-freedom structure (different from – and slightly generalizing – that found by [ZAC 11]), an example that shows that the previously investigated systems are elements of a broad set of structures behaving in a, perhaps, "unexpected way". Moreover, we present a simple generalization of a single-degree-of-freedom system, further revealing the effects of the constraint's

---

Chapter written by Davide BIGONI, Diego MISSERONI, Giovanni NOSELLI and Daniele ZACCARIA.

curvature analyzed by Bigoni *et al.* [BIG 12b]. The presence of an additional spring has an important effect on the post-critical behavior, so that two configurations (in addition to the trivial one) corresponding to a null external force are found.

Finally, we reconsider the frictional instability setup analyzed by Bigoni and Noselli [BIG 11], where a follower tangential load is transmitted by friction at a freely rotating wheel mounted at the end of a Ziegler pendulum [ZIE 77]. The application of a follower tangential load to a structure was a problem previously unsolved [ELI 05, KOI 96], but important from both a theoretical (see, for instance, [KIR 10]) and applicative point of view (for instance, to energy harvesting [DOA 11]). Within the same setting considered by Bigoni and Noselli [BIG 11], we now analyze the effects on dynamics of the inertia of the wheel and we show that, for the values of inertia pertinent to the experimental setting used, these effects are negligible, so that previous results are now fully confirmed.

1.2. Buckling in tension

Structures buckling under tensile dead loading (without elements subject to compression) were discovered by Zaccaria *et al.* [ZAC 11], who pointed out the simple example of the single-degree-of-freedom system as shown in Figure 1.1.

They also developed the concept by replacing the rigid rods with deformable elements. Though the finding by Zaccaria *et al.* [ZAC 11] might seem an isolated case, we state, on the contrary, that a broad class of structures buckling in tension can be invented. To substantiate this statement, we provide, as an example, the new single-degree-of-freedom system as shown in Figure 1.2, where two rigid rods are connected through a roller constrained to slide orthogonally to the left rod.

For this structure, bifurcation load and equilibrium paths can be calculated by considering the bifurcation mode illustrated in Figure 1.2 and defined by the rotation angle ϕ. The elongation of the system and the total potential energy are, respectively,

$$\Delta = l\left(\frac{1}{\cos\phi} - 1\right), \quad W(\phi) = \frac{1}{2}k\,\phi^2 - Fl\left(\frac{1}{\cos\phi} - 1\right), \qquad [1.1]$$

so that the force at equilibrium satisfies

$$F = \frac{k\,\phi\,\cos^2\phi}{l\sin\phi}. \qquad [1.2]$$

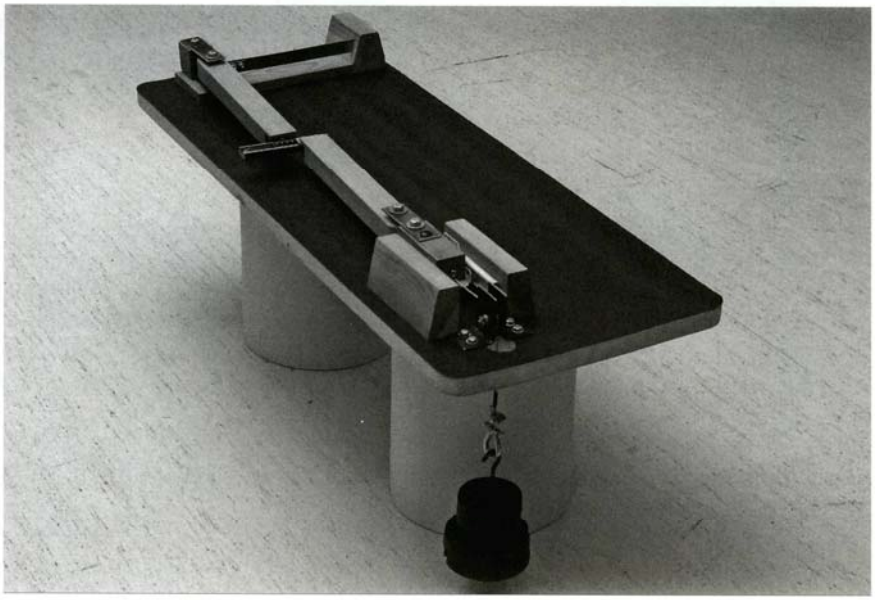

Figure 1.1. *A single-degree-of-freedom structural model showing bifurcation under tensile dead loading, where two rigid rods are connected through a slider [ZAC 11]*

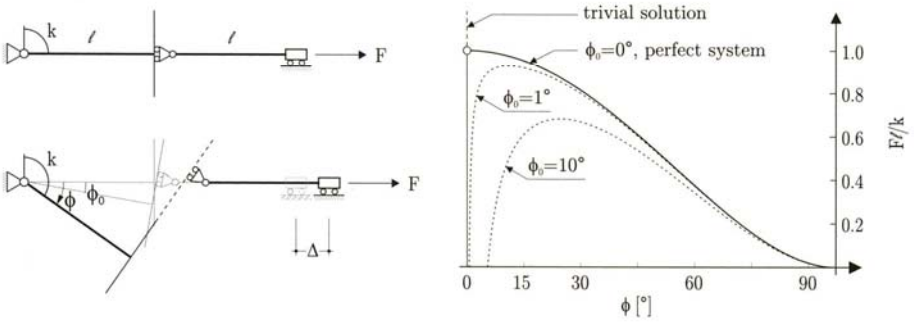

Figure 1.2. *Bifurcation of a single-degree-of-freedom elastic system under tensile dead loading (the rods of length l are rigid and connected through a roller constrained to smoothly slide along the line orthogonal to the rigid rod on the left). A rotational elastic spring of stiffness k, attached to the hinge on the left, provides the elastic stiffness. The bifurcation diagram showing bifurcation and softening in tension is reported on the right, where the angle $\phi_0 = \{1°, 10°\}$ denotes an initial imperfection*

Analysis of the second-order derivative of the strain energy reveals that the trivial solution is stable up to the critical load $F_{cr} = k/l$, while the non-trivial path, *evidencing softening*, is unstable. For an imperfect system, characterized by an initial inclination of the rods ϕ_0, we obtain

$$W(\phi, \phi_0) = \frac{1}{2}k\,(\phi - \phi_0)^2 - Fl\left(\frac{1}{\cos\phi} - \frac{1}{\cos\phi_0}\right),$$
$$F = \frac{k\,(\phi - \phi_0)\,\cos^2\phi}{l\sin\phi}, \qquad [1.3]$$

so that the force–rotation relation, shown by the dashed line in Figure 1.2 for $\phi_0 = 1°$ and $\phi_0 = 10°$, is obtained.

1.3. The effect of constraint's curvature

The strong effects related to the curvature of the profile on which a structure end is constrained to slide have been highlighted by Bigoni *et al.* [BIG 12b], who showed how to exploit a constraint to induce two critical loads (one in tension and one in compression) in a single-degree-of-freedom elastic structure. This structure, as shown in Figure 1.3, can be easily generalized by including an additional elastic spring on the hinge sliding along the profile, as shown in Figure 1.4.

In this structure, the constraint is assumed to be smooth and described in the x_1–x_2 reference system as $x_2 = l\,f(\psi)$, with $\psi = x_1/l \in [0, 1]$ and $f'(0) = 0$.

Bifurcation loads can be calculated by considering a deformed mode defined by the rotation angle ϕ, assumed to be positive when clockwise. The potential energy of the system is

$$W(\phi) = \frac{1}{2}k_1\phi^2 + \frac{1}{2}k_2\beta(\phi)^2 - F\,l\,[\cos\phi - f(\sin\phi)], \qquad [1.4]$$

so that the axial force at equilibrium becomes

$$F = -\frac{k_1\phi + k_2\,\beta(\phi)\,\beta'(\phi)}{l[\sin\phi + \cos\phi\,f'(\sin\phi)]}. \qquad [1.5]$$

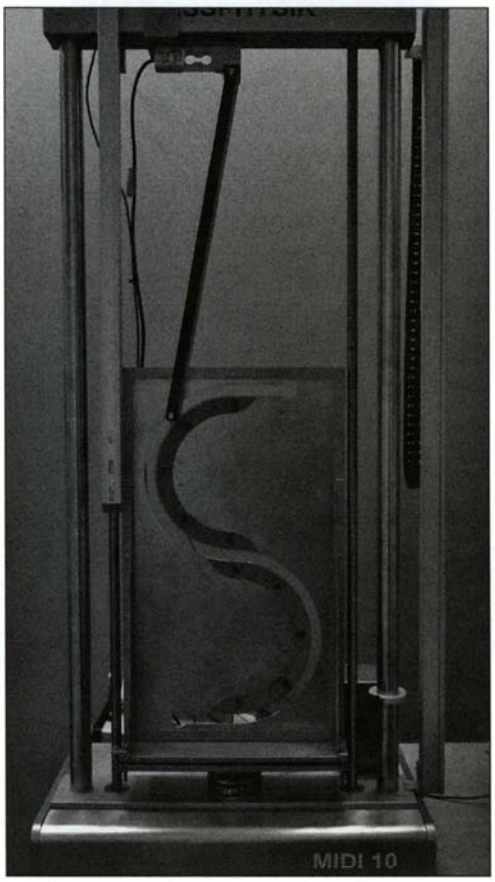

Figure 1.3. *Post-critical behavior in tension of a single-degree-of-freedom structure. The structure has two critical loads, one in tension and one in compression [BIG 12b]*

When the profile of the constraint is circular, with radius R_c and dimensionless signed curvature $\widehat{\chi} = f''/[1+(f')^2]^{3/2} = \pm l/R_c$ as shown in the inset of Figures 1.5 and 1.6, the axial load at equilibrium satisfies

$$F = -\frac{k_1\phi\sqrt{1-\widehat{\chi}^2\sin^2\phi}}{l\sin\phi(\widehat{\chi}\cos\phi+\sqrt{1-\widehat{\chi}^2\sin^2\phi})} + \\ -\frac{k_2\left[\phi+\sin^{-1}(\widehat{\chi}\sin\phi)-\pi\,\mathrm{H}(\widehat{\chi}\,\phi)\right]}{l\sin\phi}, \qquad [1.6]$$

where H denotes the Heaviside step function. Since $\beta(\phi) = -\tan^{-1}[f'(\sin\phi)] - \phi$, the critical load of the system is

$$F_{cr} = -\frac{k_1 + k_2\,[1 + f''(0)]^2}{l[1 + f''(0)]} \qquad [1.7]$$

where $f''(0) = \widehat{\chi}(0)$ is the signed curvature at $\phi = 0$.

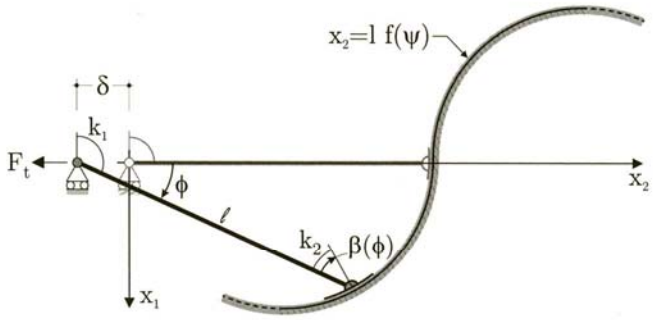

Figure 1.4. *A single-degree-of-freedom structure with a linear-elastic hinge constrained to slide along a generic profile at the right end and a rotational linear-elastic spring at the left end*

For an imperfect system, characterized by an initial inclination of the rod ϕ_0, the potential energy becomes

$$\begin{aligned} W(\phi) =& \frac{1}{2}k_1(\phi - \phi_0)^2 + \frac{1}{2}k_2\,[\beta(\phi) - \beta(\phi_0)]^2 + \\ & - F\,l\,[\cos\phi - f(\sin\phi) - \cos\phi_0 + f(\sin\phi_0)]\ , \end{aligned} \qquad [1.8]$$

so that the axial force at equilibrium is

$$F = -\frac{k_1(\phi - \phi_0) + k_2\ [\beta(\phi) - \beta(\phi_0)]\ \beta'(\phi)}{l[\sin\phi + \cos\phi\, f'(\sin\phi)]}, \qquad [1.9]$$

which for a circular profile becomes

$$\begin{aligned} F = & -\frac{k_1(\phi - \phi_0)\sqrt{1 - \widehat{\chi}^2\sin^2\phi}}{l\sin\phi(\widehat{\chi}\cos\phi + \sqrt{1 - \widehat{\chi}^2\sin^2\phi})} + \\ & -\frac{k_2\big[\phi - \phi_0 + \sin^{-1}(\widehat{\chi}\sin\phi) + \mathrm{sign}(\widehat{\chi}\,\phi)\sin^{-1}(\widehat{\chi}\sin\phi_0) - \pi\,\mathrm{H}(\widehat{\chi}\,\phi)\big]}{l\sin\phi}\ . \end{aligned} \qquad [1.10]$$

Equation [1.10] has been used for $\widehat{\chi} = \pm 4$, with an "S-shaped" constraint (so that $\widehat{\chi}$ is discontinuous at $\phi = 0$), to obtain the results shown in Figures 1.5 and 1.6.

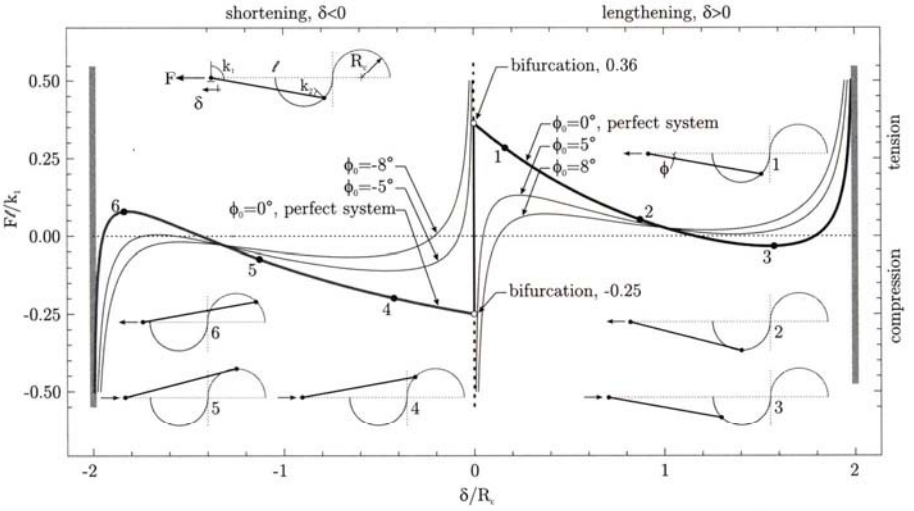

Figure 1.5. *The force versus end displacement behavior of a single-degree-of-freedom structure, with an "S-shaped" constraint, $\widehat{\chi} = \pm 4$ and $k_2/k_1 = 0.01$, evidencing two buckling loads, one compressive and one tensile. Note the four points where the force vanishes*

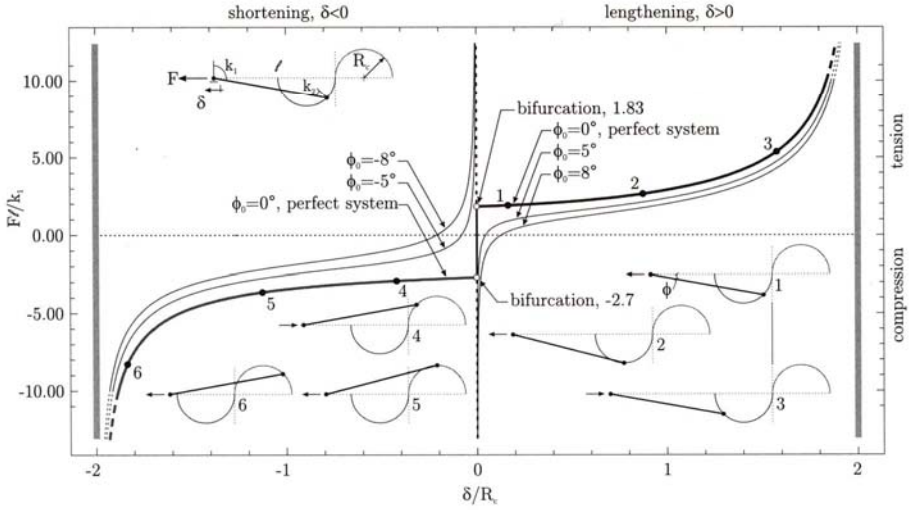

Figure 1.6. *The force versus end displacement behavior of a single-degree-of-freedom structure, with an "S-shaped" constraint, $\widehat{\chi} = \pm 4$ and $k_2/k_1 = 0.5$, evidencing two buckling loads, one compressive and one tensile. Note that at points labelled "2" and "5", the external force does not vanish*

1.4. The Ziegler pendulum made unstable by Coulomb friction

The first experimental evidence of *flutter* and *divergence* instability related to dry friction has recently been provided by Bigoni and Noselli [BIG 11]. In their experimental study, essentially based on the Ziegler's double pendulum [ZIE 77], Coulomb friction was exploited in order to provide the system with a tangential follower force of frictional origin. This goal was achieved by endowing the double pendulum with a freely rotating wheel, constrained to slide with friction on a horizontal plate (see Figure 1.7 for the experimental setting and Figure 1.8 for a sequence of images revealing flutter instability).

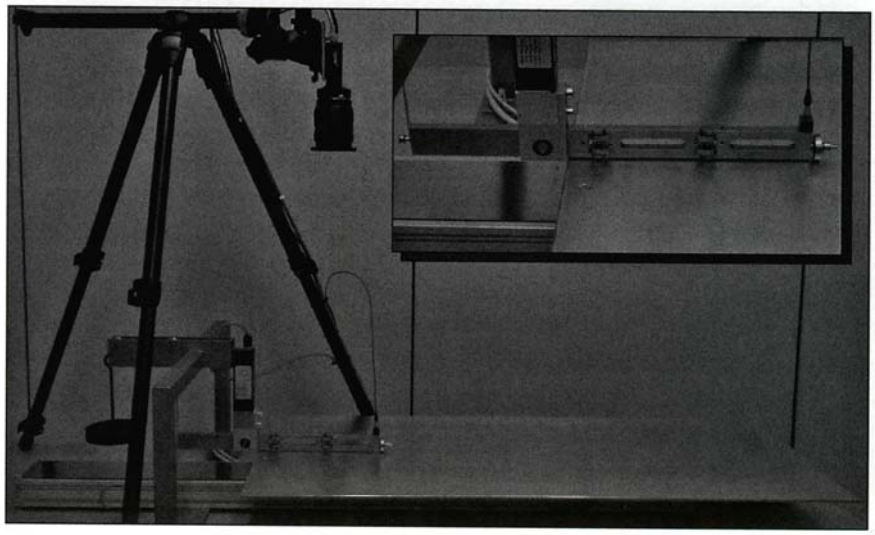

Figure 1.7. *The experimental setting used by Bigoni and Noselli [BIG 11] to show the connection between Coulomb friction and dynamic instabilities such as flutter and divergence. A Ziegler double pendulum is endowed at its tip with a freely rotating wheel, constrained to slide on a horizontal plate and providing the system with a follower force of frictional origin*

Note that, to generate a force of the frictional type, a transversal reaction between plate and wheel is needed, which during the experiments was created by hanging a dead weight W on the left of the structure, used as a lever.

In their experimental study, Bigoni and Noselli [BIG 11] analyzed the stability of the double pendulum using the five different wheels, as shown in Figure 1.9; however, in their numerical analyses, the wheel was assumed to be massless, so the aim of this section is to show the effects on the system's dynamic of a heavy wheel.

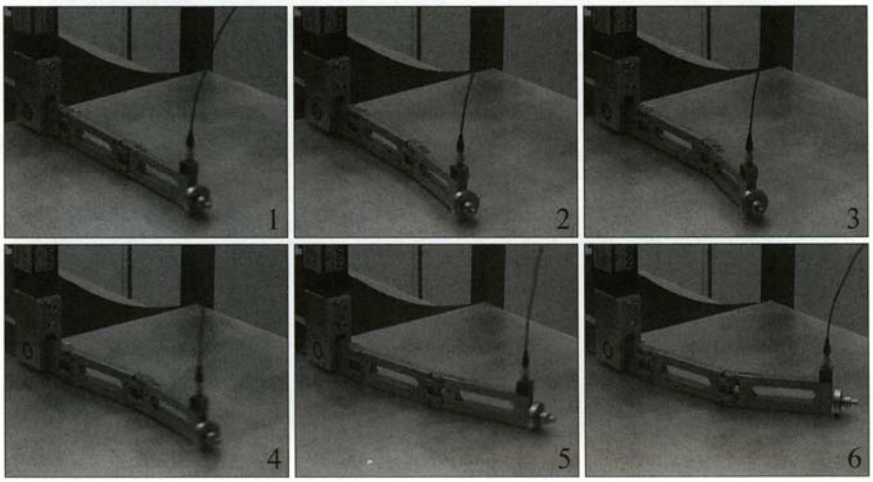

Figure 1.8. *A sequence of images (taken from a movie recorded with a Sony handycam at 25 frames per second) of the structure shown in Figure 1.7 and exhibiting flutter instability. The whole sequence of images was recorded in 0.40 s and the time interval between two images was 0.08 s*

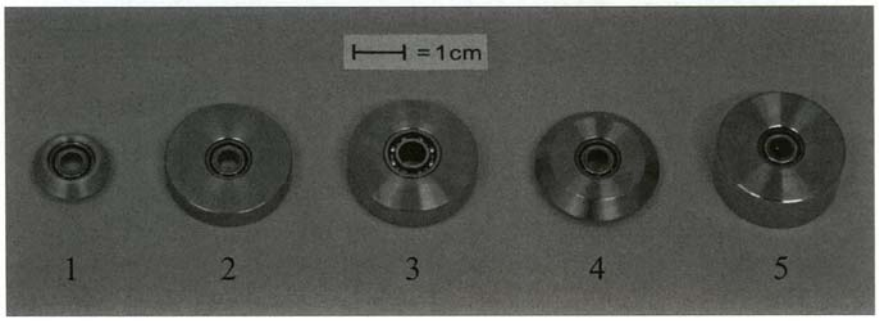

Figure 1.9. *The five different wheels used in the experimental tests by Bigoni and Noselli [BIG 11]. (1) Aluminum wheel with V-shaped cross-section, external diameter 15 mm, thickness 5 mm, weight 3 g; (2) cylindrical steel wheel, external diameter 25 mm, thickness 5 mm, weight 18 g; (3) cylindrical steel wheel, external diameter 25 mm, thickness 6 mm weight 22 g; (4) steel wheel with V-shaped cross-section, external diameter 25 mm, thickness 6 mm, weight 17 g; (5) cylindrical steel wheel, external diameter 25 mm, thickness 10 mm, weight 36 g*

When the mass of the wheel is taken into account, this is subject to a radial ($\mathbf{e}_r = \cos\alpha_2\,\mathbf{e}_1 + \sin\alpha_2\,\mathbf{e}_2$) force $\mathbf{P}$ and to a tangential ($\mathbf{e}_t = -\sin\alpha_2\,\mathbf{e}_1 + \cos\alpha_2\,\mathbf{e}_2$) force

$\mathbf{T}$ applied at the contact point with the moving plate as shown in Figure 1.10. These forces can be expressed in component form as

$$\begin{aligned} \mathbf{P} &= -P\cos\alpha_2\,\mathbf{e}_1 - P\sin\alpha_2\,\mathbf{e}_2\,, \\ \mathbf{T} &= -T\sin\alpha_2\,\mathbf{e}_1 + T\cos\alpha_2\,\mathbf{e}_2\,. \end{aligned} \qquad [1.11]$$

where the two scalar quantities P and T have been introduced. Note that P and T are positive quantities when the forces acting on the wheel are directed as in Figure 1.10, and, in general, their absolute values equal to $|\mathbf{P}|$ and $|\mathbf{T}|$, respectively.

The assumption of Coulomb friction at the contact point between the wheel and the plate allows us to write

$$P = \begin{cases} \text{sign}(\dot{C}_p^r)\sqrt{(\mu_d\,R)^2 - T^2} & \text{if } \dot{C}_p^r \neq 0\,, \\ \left[-\sqrt{(\mu_s\,R)^2 - T^2},\ \sqrt{(\mu_s\,R)^2 - T^2}\right] & \text{if } \dot{C}_p^r = 0\,,\quad \dot{C}_p^t + \dot{\alpha}_3\,r_w = 0\,, \\ 0 & \text{if } \dot{C}_p^r = 0\,,\quad \dot{C}_p^t + \dot{\alpha}_3\,r_w \neq 0\,, \end{cases} \qquad [1.12]$$

where R is the vertical reaction applied at the wheel and orthogonal to the moving plane, μ_s and μ_d are the static and dynamic friction coefficients, respectively, and $\dot{C}_p^r$ and $\dot{C}_p^t$ are the radial and the tangential components of the velocity of the wheel with respect to the plate, which can be expressed in the forms

$$\begin{aligned} \dot{C}_p^r &= v_p\,\cos\alpha_2 - l_1\sin(\alpha_1 - \alpha_2)\dot{\alpha}_1\,, \\ \dot{C}_p^t &= -v_p\,\sin\alpha_2 + l_1\cos(\alpha_1 - \alpha_2)\dot{\alpha}_1 + l_2\dot{\alpha}_2\,. \end{aligned} \qquad [1.13]$$

The system is characterized by three-degrees-of-freedom, denoted by α_1, α_2 and α_3, and the latter representing the rotation of the wheel about its axis (see Figure 1.10). Moreover, m_w, r_w and h_w are the mass, the radius and the thickness of the wheel.

The principle of virtual works, denoting the scalar product with " $\cdot$ ", is written as

$$\begin{aligned} &\mathbf{P}\cdot\delta\mathbf{C} + \mathbf{T}\cdot(\delta\mathbf{C} + r_w\delta\alpha_3\,\mathbf{e}_t) - (k_1\alpha_1 + \beta_1\dot{\alpha}_1)\delta\alpha_1 + \\ &- [k_2(\alpha_2 - \alpha_1) + \beta_2(\dot{\alpha}_2 - \dot{\alpha}_1)](\delta\alpha_2 - \delta\alpha_1) + \\ &- m_1\ddot{\mathbf{G}}_1\cdot\delta\mathbf{G}_1 - m_2\ddot{\mathbf{G}}_2\cdot\delta\mathbf{G}_2 - m_w\ddot{\mathbf{C}}\cdot\delta\mathbf{C} + \\ &- I_{13}\,\ddot{\alpha}_1\delta\alpha_1 - I_{23}\,\ddot{\alpha}_2\delta\alpha_2 - I_{w_r}\,\ddot{\alpha}_3\delta\alpha_3 - I_{w3}\,\ddot{\alpha}_2\delta\alpha_2 = 0, \end{aligned} \qquad [1.14]$$

holding for every virtual displacement $\delta\mathbf{C}$, $\delta\mathbf{G}_1$ and $\delta\mathbf{G}_2$, functions of the virtual rotations $\delta\alpha_1$, $\delta\alpha_2$ and $\delta\alpha_3$.

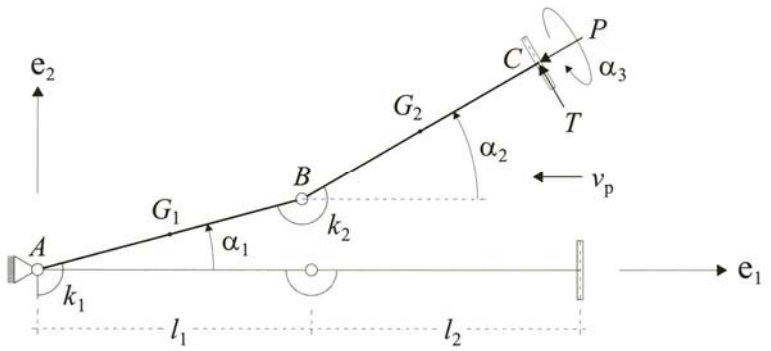

Figure 1.10. *A three-degree-of-freedom system subject to a tangential follower force* $\mathbf{P}$ *and orthogonal follower force* $\mathbf{T}$ *provided by a freely rotating wheel sliding with friction on a plate, which moves with velocity of modulus* v_p*. The two rods, of linear mass density* ρ*, are rigid and connected through two rotational springs of stiffness* k_1 *and* k_2 *and viscosity* β_1 *and* β_2*. The wheel has mass* m_w*, radius* r_w *and thickness* h_w

In equation [1.14], m_1, m_2 and m_w are, respectively, the mass of the rod of length l_1, the mass of the rod of length l_2 and the mass of the wheel, whereas I_{13}, I_{23}, I_{w3} and I_{wr} are, respectively, the principal moment of inertia of the two rods about the vertical axis and the principal moment of inertia of the wheel about the vertical axis and its rotation axis.

Now imposing condition [1.14] and invoking the arbitrariness of $\delta\alpha_1$, $\delta\alpha_2$ and $\delta\alpha_3$, we arrive at the system of three nonlinear differential equations, governing the dynamics of the system

$$
\begin{cases}
[I_{13} + l_1^2(m_1/4 + m_2 + m_w)]\ddot{\alpha}_1 + l_1 l_2 (m_2/2 + m_w)\cos(\alpha_1 + \alpha_2)\ddot{\alpha}_2 + \\
+ \beta_1\dot{\alpha}_1 + \beta_2(\dot{\alpha}_1 - \dot{\alpha}_2) + k_1\alpha_1 + k_2(\alpha_1 - \alpha_2) + \\
+ l_1 l_2 (m_2/2 + m_w)\sin(\alpha_1 - \alpha_2)\dot{\alpha}_2^2 + \\
- l_1[T\cos(\alpha_1 - \alpha_2) + P\sin(\alpha_1 - \alpha_2)] = 0, \\
\\
l_1 l_2 (m_2/2 + m_w)\cos(\alpha_1 - \alpha_2)\ddot{\alpha}_1 + [I_{23} + I_{w3} + l_2^2(m_2/4 + m_w)]\ddot{\alpha}_2 + \\
- \beta_2(\dot{\alpha}_1 - \dot{\alpha}_2) - k_2(\alpha_1 - \alpha_2) + \\
- l_1 l_2 (m_2/2 + m_w)\sin(\alpha_1 - \alpha_2)\dot{\alpha}_1^2 - l_2\, T = 0, \\
\\
I_{wr}\,\ddot{\alpha}_3 - r_w\, T = 0\,.
\end{cases}
\qquad [1.15]
$$

We note from equations [1.12]–[1.15] that α_1, α_2, α_3, P and T are the five unknowns, function of time. Moreover, in the case in which sliding between the wheel and the plate is active, a situation corresponding to $\dot{C}_p^{r} \neq 0$, one additional condition has to be imposed in order to find the solution, namely, that the force applied to the wheel, $\mathbf{P} + \mathbf{T}$, must be directed parallel, but opposite to the relative plate/wheel velocity, $\dot{\mathbf{C}} + v_p\,\mathbf{e}_1 + \dot{\alpha}_3\, r_w\,\mathbf{e}_t$, a condition yielding

$$\frac{P}{T} = \frac{v_p \cos\alpha_2 - l_1 \sin(\alpha_1 - \alpha_2)\dot{\alpha}_1}{v_p \sin\alpha_2 - l_1 \cos(\alpha_1 - \alpha_2)\dot{\alpha}_1 - l_2\dot{\alpha}_2 - r_w\,\dot{\alpha}_3}. \qquad [1.16]$$

The nonlinear system of equations has been numerically solved, and for this purpose the function "NDSolve" of Mathematica 6.0 has been used, together with a viscous smooth approximation of the friction law [1.12] (see [ODE 85, BIG 11]).

In Figure 1.11, a comparison is found (in terms of α_1 and α_2) between the numerical results for the case of a massless (solid curves) and a heavy (dashed curve) wheel. These results have been obtained for a dead weight W corresponding to the onset of flutter instability and assuming wheel number 3 as shown in Figure 1.9. From the results shown in Figure 1.11, we can conclude that the inertia of the wheel only slightly contributes to the motion of the system and can therefore be neglected.

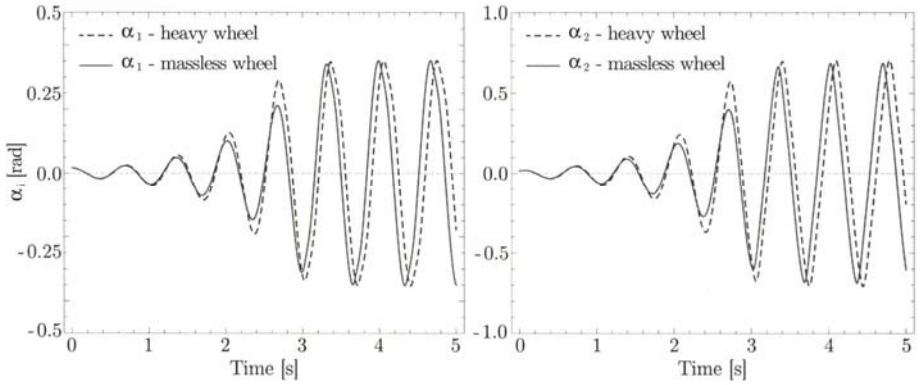

Figure 1.11. *The instantaneous rotations α_1 and α_2 of the Ziegler pendulum's rods, numerically obtained as functions of time, for massless (solid curves) and heavy (dashed curves, the assumed wheel is number 3 in Figure 1.9) wheels. The results have been obtained for a dead load W at the onset of flutter, a plate velocity v_p = 50 mm/s and initial conditions $\alpha_1 = \alpha_2 = 1^\circ$*

1.5. Conclusions

Instability in tension, effects of a constraint's curvature and follower loads induced by dry Coulomb friction are new phenomena that open an important perspective in the design of structures that can become unstable at prescribed loads.

New examples of structures exhibiting buckling under tensile dead loading have been given, slightly generalizing previous findings by the authors and showing that a broad set of systems behaving in a counterintuitive and innovative way can be invented and practically realized.

The effects of a constraint's curvature have been further investigated: we have shown that the introduction on a curved constraint profile of an elastic, torsional spring strongly affects the post-critical behavior of the system and may lead to multiple equilibrium configurations, corresponding to an external force of zero magnitude.

Finally, we have presented also a detailed analysis of flutter instability as induced by dry friction in the Ziegler double pendulum. In this system, dynamical effects related to a heavy frictional constraint have been determined. The results show that these are negligible for the values of a constraint's inertia pertinent to our experimental setting, but may become interesting in other situations.

The structures considered in our study can be combined to design flexible systems and artificial materials, which may find broad applications, even at the micro- and nanoscale.

1.6. Acknowledgments

Financial support from the European FP7 – Intercer2 project (PIAP-GA-2011-286110-INTERCER2) is gratefully acknowledged.

1.7. Bibliography

[BIG 11] BIGONI D., NOSELLI G., "Experimental evidence of flutter and divergence instabilities induced by dry friction", *Journal of the Mechanics and Physics of Solids*, vol. 59, no. 10, pp. 2208–2226, 2011.

[BIG 12a] BIGONI D., *Nonlinear Solid Mechanics. Bifurcation Theory and Material Instability*, Cambridge University Press, 2012.

[BIG 12b] BIGONI D., MISSERONI D., NOSELLI G., *et al.*, "Effects of the constraint's curvature on structural instability: tensile buckling and multiple bifurcations", *Proceedings of the Royal Society A: Mathematical, Physical and Engineering Sciences*, vol. 468, no. 2144, pp. 2191–2209, 2012.

[DOA 11] DOARE O., MICHELIN S., "Piezoelectric coupling in energy-harvesting fluttering flexible plates: linear stability analysis and conversion efficiency", *Journal of Fluids and Structures*, vol. 27, no. 8, pp. 1357–1375, 2011.

[ELI 05] ELISHAKOFF I., "Controversy associated with the so-called 'follower force': critical overview", *Applied Mechanics Reviews*, vol. 58, no. 2, pp. 117–142, 2005.

[KIR 10] KIRILLOV O.N., VERHULST F., "Paradoxes of dissipation-induced destabilization or who opened Whitney's umbrella?", *Zeitschrift für Angewandete Mathematik und Mechanik*, vol. 90, no. 6, pp. 462–488, 2010.

[KOI 96] KOITER W.T., "Unrealistic follower forces", *Journal of Sound and Vibration*, vol. 194, no. 4, pp. 636–638, 1996.

[ODE 85] ODEN J.T., MARTINS J.A.C., "Models and computational methods for dynamic friction phenomena", *Computer Methods in Applied Mechanics and Engineering*, vol. 52, no. 1–3, pp. 527–634, 1985.

[SUG 95] SUGIYAMA Y., KATAYAMA K., KINOI S., "Flutter of a cantilevered column under rocket thrust", *Journal of Aerospace Engineering*, vol. 8, no. 1, pp. 9–15, 1995.

[ZAC 11] ZACCARIA D., BIGONI D., NOSELLI G., *et al.*, "Structures buckling under tensile dead load", *Proceedings of the Royal Society A: Mathematical, Physical and Engineering Sciences*, vol. 467, no. 2130, pp. 1686–1700, 2011.

[ZIE 77] ZIEGLER H., *Principles of Structural Stability*, Birkhäuser Verlag, Basel, Stuttgart, 1977.